Underground Ventilation – Tukkaraja (Ed)
© 2023 The Author(s), ISBN 978-1-032-55146-3

Analysis of variation in longwall-induced permeability under different mining depths

Kayode M. Ajayi, Zoheir Khademian, Steven J. Schatzel, Marcia L. Harris & James D. Addis
Centers for Disease Control and Prevention, National Institute for Occupational Safety and Health, Pittsburgh, PA, USA

ABSTRACT: Longwall-induced deformation could compromise the stability of shale gas wells positioned in the abutment pillars of current and future coal reserves. Consequently, gas from the casing(s) could flow towards the mine increasing the risk of explosive gas accumulation beyond the mandated limits. To assess the impact of this hypothetical scenario, the permeabilities of the surrounding strata are required to be quantified for potential gas flow to the mine. However, varying mining depths for different coal reserves could significantly impact permeability. Therefore, this study presents an analysis of longwall-induced permeability under shallow, <152 m (<500 feet), and deep cover, >274 m (>900 feet), using measurements obtained from different study sites in southwestern Pennsylvania along with discrete fracture network (DFN) modeling in 3DEC and Fracture Flow Code (FFC). The field study measured permeability changes for specific strata, and the numerical model predicted the permeability changes for all the strata in the overburden. At the study site, the maximum permeability measured over the abutment pillar at the Uniontown horizon is 2.17×10^{-14} m^2 (22 mD) and 1.75×10^{-14} m^2 (18 mD) for deep and shallow cover sites, respectively. These findings provide a measure for comparing the potential risk of a hypothetical breach under a shallow and a deep cover.

1 INTRODUCTION

The integrity of an unconventional shale gas well positioned in the abutment pillar of a longwall mine could be compromised due to mining-induced deformation. Consequently, gas from the compromised casing(s) is released in the overburden and could flow towards the mine. This increases the risk of an explosion or accumulation of explosive gas beyond the mandated limits (Mine Safety and Health Administration, 2018). This is a novel problem as the coexistence of coal and shale gas is an emerging field in current and future coal reserves in Pennsylvania, West Virginia, Ohio, Virginia, and Tennessee. Currently, it is required that shale gas wells near mining should be plugged or adequately protected by a designed pillar following the design criteria developed from the 1957 Pennsylvania Gas Well Pillar Study (Commonwealth of Pennsylvania, 1957), which predates longwall mining. This current study requires an update to consider new mining methods such as longwall mining and the impact of deep-cover mining. Hence, researchers at the National Institute for Occupational Safety and Health (NIOSH) have been conducting research to provide engineering guidelines for shale gas wells influenced by longwall mining under shallow, medium, and deep cover. Findings from these studies have predicted and measured horizontal displacement within the abutment pillar where the unconventional gas wells are positioned (Su et al., 2019, Su et al., 2018, Zhang et al., 2019a, Zhang et al., 2019b). For a medium and deep-cover site in southwestern Pennsylvania, Su et al. (2019) predicted that the horizontal displacement under deep cover (at 361-m depth) is one order of magnitude smaller than the medium-cover site. Even though this observation might be site specific, the findings show that the impact of mining-induced deformation could vary with depth.

DOI: 10.1201/9781003429241-52

The Pennsylvania longwall mine data shows that mining depth could be as shallow as 30.48 m (100 ft) in stream locations and as deep as 366 m (1,200 ft) (Pennsylvania Department of Environmental Protection, 2022). Similarly, the depth of the target Marcellus Shale could vary from 1,500 to 2,700 m (Zhang et al., 2019b). Therefore, these unconventional shale gas wells have been drilled through coal seams, and the impact of mining-induced deformation on the gas well casing could vary due to the mining depth. Even though the current research by NIOSH is aimed at providing engineering principles to ensure a safe co-existence of both operations (coal mining and shale gas extraction), it is also important to consider the impact of a hypothetical shale gas well casing breach. The possibilities that the gas could flow towards the mine is dependent on the permeability of the surrounding strata from the breach location to the mine. Schatzel et al. (2012) observed that mining-induced permeability could change up to 7 months after mining with a hundred or thousands millidarcy increase. Hence, this research group has conducted field studies to measure mining-induced permeability at study sites in southwestern Pennsylvania under shallow and deep cover (Watkins et al., 2021). Due to the limitations of field studies in the number of strata that could be monitored, a discrete fracture network (DFN) model was developed using the core log data of the study sites (Ajayi et al., 2022, Khademian Z. et al., 2022). DFN models are preferred because the fractures are modelled explicitly similar to field conditions unlike the continuum approach. It assumes that the fracture permeabilities are notably greater than the permeability of the rock matrix such that it can be ignored . The model is stochastic because it is impractical to exactly represent the fracture network in the overburden. It is used to predict the permeability of all the strata in the overburden, and the results are validated with the field measurements. Previous numerical models for a shallow-cover site (Ajayi et al., 2021) and a deep-cover site (Khademian Z. et al., 2022) have focused on the permeability over the abutment pillar. However, this study presents the permeability for the overburden from the center of the abutment pillar to the gob (Figure 1). The difference in the induced permeability is used to analyze the impact of a hypothetical casing breach on the mine under different covers. The research approach is presented in Section 2.0 and the findings are presented in Section 3.0 with conclusions in Section 4.0.

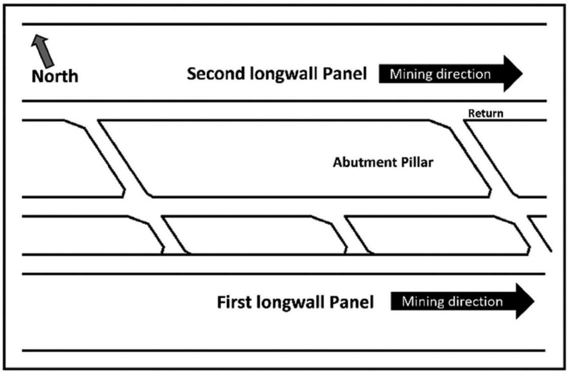

Figure 1. Layout of the first and second panel.

2 RESEARCH APPROACH

2.1 *Field study and site geology*

Figure 2 summarizes the method used in this study to predict mining-induced permeability for a shallow and deep-cover site in southwestern Pennsylvania. Both sites are mining the Pittsburgh coal bed in the Northern Appalachian Basin using the longwall mining method. Both sites have two adjacent longwall panels with a width of 457.2 m (1,500 ft) each with a three-entry gateroad system, and a 38.1-m × 83.82-m (125-ft × 275-ft) center abutment pillar as illustrated in Figure 2. The lithology of the overburden consists of mainly sandstone, sandy shale, limestone, shale, coal, and shaley limestone. The mining horizon for the shallow-cover site is 146.9-m (482-ft) and four monitoring boreholes were drilled over the abutment pillar. Three of the boreholes monitored mining-induced permeability changes during the mining of both panels, and the fourth borehole monitored the ground movement due to longwall mining. The boreholes monitored permeability changes at specific horizons: the first borehole (tagged FEB 1) monitored the Sewickley coal horizon at 124.97-m (410-ft) depth, the second borehole (tagged FEB 2) monitored the Uniontown coal horizon monitored at 79.29-m (260-ft) depth, and the third borehole (tagged FEB 3) monitored 41.15-m (135-ft) depth, which targets the projected top of the fractured zone. The choice of these monitoring locations is based on an earlier geomechanical study for the shallow-cover site, which identified that the Sewickley and Uniontown horizons are the primary zones of horizontal displacement of 17 cm and 4 cm, respectively. The deep cover site is a longwall mine with an overburden depth of 341 m (1,119 ft). Tables 1 and 2 present a summary of the field permeability measurements conducted using a falling-head test for the shallow and deep-cover sites, respectively.

Table 1. Field permeability measurements over the abutment pillar for shallow cover (Watkins E, 2020).

Borehole ID	First Panel Range m^2 (mD)	Second Panel Range m^2 (mD)
FEB 1	$4.07 \times 10^{-13} - 1.35 \times 10^{-12}$ (411–1,360)	$1.09 \times 10^{-12} - 5.03 \times 10^{-12}$ (1,100–5080)
FEB 2	$2.17 \times 10^{-14} - 2.43 \times 10^{-13}$ (21.9–245)	$1.14 \times 10^{-14} - 3.82 \times 10^{-13}$ (11.5–386)
FEB 3	$2.70 \times 10^{-12} - 3.26 \times 10^{-11}$ (2,730–32,900)	$3.81 \times 10^{-11} - 1.31 \times 10^{-10}$ (38,500–132,000)

Table 2. Permeability measurements over the gob for deep cover (Khademian Z. et al., 2022).

Borehole ID	Location	First Panel Range m^2 (mD)
Pre-mining-Borehole A	295-m depth and 98 m away from the tailgate gateroad	$2.42 \times 10^{-13} - 2.81 \times 10^{-13}$ (245-285)
Post Mining-Borehole B	265-m depth at the Uniontown coal horizon and at the center of the mined panel	$6.61 \times 10^{-14} - 1.21 \times 10^{-13}$ (67- 123)
VEP-S	370 m depth at the Sewickley coal horizon (328 m) and over the abutment pillar	$4.64 \times 10^{-16} - 1.75 \times 10^{-14}$ (0.47-17.73)
VEP-U	370 m depth at the Uniontown coal horizon (291 m) and over the abutment pillar	$1.84 \times 10^{-16} - 5.33 \times 10^{-15}$ (0.19-5.4)

2.2 *Geomechanical model for aperture prediction*

The permeability of rock mass surrounding the gas well is required to quantify the flow of shale gas from a hypothetical breach location to the mining area. Khademian et al. (2022) developed a geomechanical modeling methodology for estimating fracture aperture changes due to longwall mining. This approach was based on the DFN technique for explicitly modeling fractures in rock using 3-Dimensional Distinct Element Method (3DEC) software and calculating their apertures affected by longwall stress and deformations. A shallow, 145-m-cover mine in the Pittsburgh coal seam was used to calibrate the mechanical and hydraulic properties of fractures using pre-mining permeability measurements, post-mining pillar stress, and surface subsidence. The same calibration parameters were used in a deep-cover (341-m) longwall mine in southwestern Pennsylvania in the Pittsburgh coal bed, and the modeled permeability results were shown to agree reasonably with the field permeability measurements. The calibrated properties of fractures were fracture friction coefficients being 60% of the strata internal friction, initial fracture apertures of 0.3–0.5 mm, fracture density (total fracture area in unit volume of rock) of 0.15 in weak coal horizon, fracture density of 0.2 for the shallow weathered zone, and fracture density of 0.3 for the interconnected fracture zone (with a height of about 23 times the mining height).

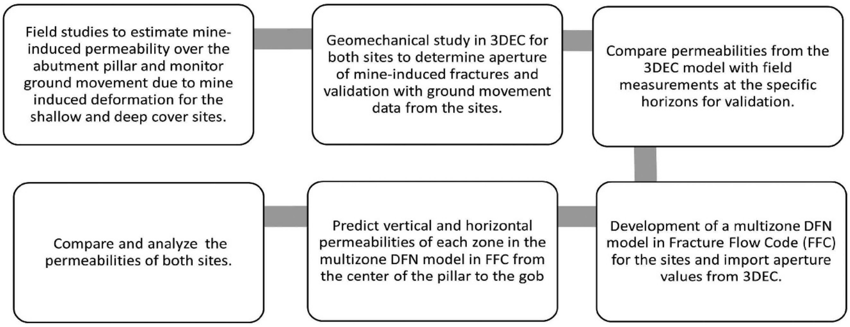

Figure 2. Summary of the research approach.

2.3 *Development of multizone DFN model and numerical model for permeability*

As described in Section 1.0 (Introduction), it is impractical to exactly represent the fractures in the overburden. Therefore, a stochastic DFN model is developed in Fracture Flow Code (FFC) to predict mining-induced permeability. In a previous study conducted with FFC, the overburden was classified into three zones: Tailgate Abutment pillar area, Gob area, and Headgate chain pillar area. However, this approach has its limitations because a mining-induced aperture could change within a short interval. Therefore, FFC is updated such that it discretizes the overburden. The region over the abutment pillar is classified into 5-m zones toward the edge of the panel, and the section over the gob is classified as 10-m zones. It is assumed that these zones completely map the exact values of the aperture value from the geomechanical model in 3DEC. Within each zone, the center location of the vertical fractures is generated using uniform distribution, the length of the fractures is modeled with lognormal distribution, the fracture density is imported from the 3DEC model, the aperture is modeled with lognormal distribution using the peak value of each zone from 3DEC, and the fracture orientation is modeled with Von Mises Fischer's distribution. The model generates 100 DFN realizations to replicate the potential variation in fracture geometries, and the average permeability is presented in this study. Figure 3 shows one of the DFN realizations of the multizone model generated in FFC for the shallow-cover site.

For each zone in Figure 3, the vertical and horizontal permeabilities are determined using the method presented in a previous study (Zhang et al., 1996). Cubic law is used to model flow through the fractures and Darcy's equation is used to predict the permeabilities (Zhang et al., 1996):

$$\begin{bmatrix} q_{xx} & q_{xy} \\ q_{yx} & q_{yy} \end{bmatrix} = \begin{bmatrix} K_{xx} & K_{xy} \\ K_{yx} & K_{yy} \end{bmatrix} \begin{bmatrix} \nabla H_x & 0 \\ 0 & \nabla H_y \end{bmatrix}. \quad (1)$$

In Equation 1, q indicates the direction of flow and velocity (m/s), and it is calculated by dividing the sum of boundary flow from cubic law (Q, $m^{3/}s$,) by the boundary area (A, m^2), ∇H_x *and* ∇H_y are the pressure head gradients in the x and y directions, respectively, and K is the permeability coefficient or conductivity (m/s). The principal (q_{yy} and q_{xx}) and cross flow (q_{xy} and q_{yx}) in the y and x directions, respectively, are obtained by applying boundary pressure independently in both directions. The absolute permeability tensor (k in m^2) is obtained from:

$$k = \frac{K\mu}{\rho g}. \quad (2)$$

ρ is the density of fluid kg/m^3, g is the acceleration due to gravity (m/s^2), μ is the dynamic viscosity of the fluid (Ns/m^2). The principal absolute permeabilities in the x (k_{xx}) and y (k_{yy}) directions are the horizontal and vertical permeabilities.

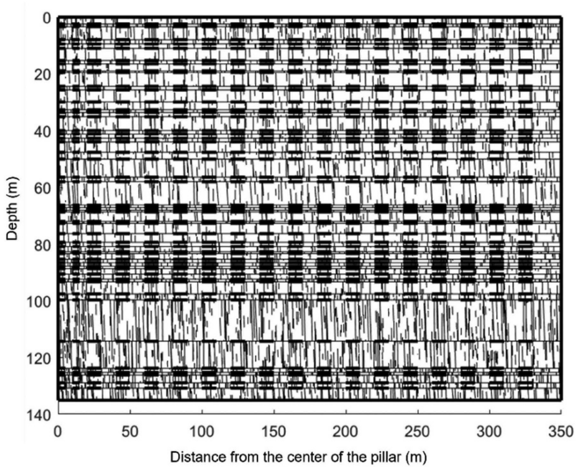

Figure 3. Stochastic DFN model generated for FFC.

3 RESULTS AND DISCUSSION

This section presents the permeability results from FFC for shallow and deep cover from the center of the abutment pillar to 350 m (1,148 ft). Even though the width of the panel is 457.2 m (1,500 ft), the choice of 350 m (1,148 ft) is to focus on the area of interest closer to the gas well in the abutment pillar and save on the computational time required for the full model. Figures 4 and 5 show the average permeability from 100 DFN realizations for each of the zones in the overburden for shallow and deep cover, respectively. These permeability maps are developed using the same range for ease of comparison.

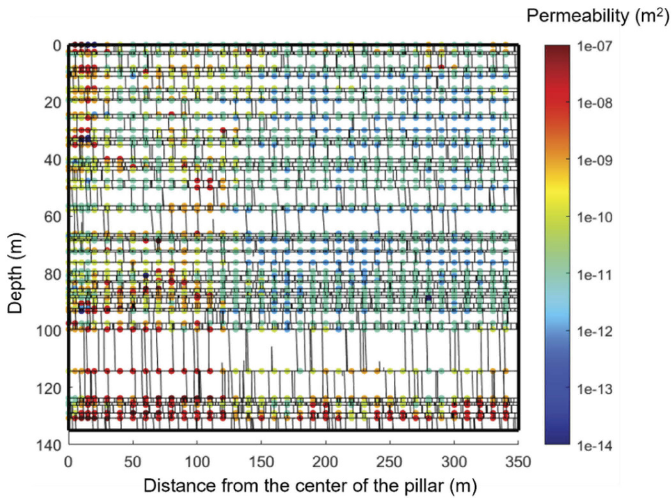

Figure 4. Permeability distribution for shallow cover.

It is observed that from the permeability map in Figure 4 that the values over the abutment pillar (within 0–15 m) are about an order of magnitude lower than the edge of the panel. For most of the strata, the permeability at the edge of the panel is highest and gradually decreases towards the gob. Under this shallow-cover condition, the impact of mining-induced deformation is significant within 100 m from the center of the panel and gradually decreases towards the gob except for the strata within 40 m from the mine roof and about 10 m from the surface. The strata directly closest to the mine roof (within 40 m) seems to have an extended higher permeability region into the gob. The lowest permeabilities are toward the center of the gob for strata between 10–100 m. Even though these observations are unique for this site, the results show that mining-induced deformation could significantly impact the overburden under shallow cover. By comparing Figures 4 and 5, the mining-induced permeability for most of the zones under deep cover in Figure 5 is significantly lower than in shallow cover (Figure 4).

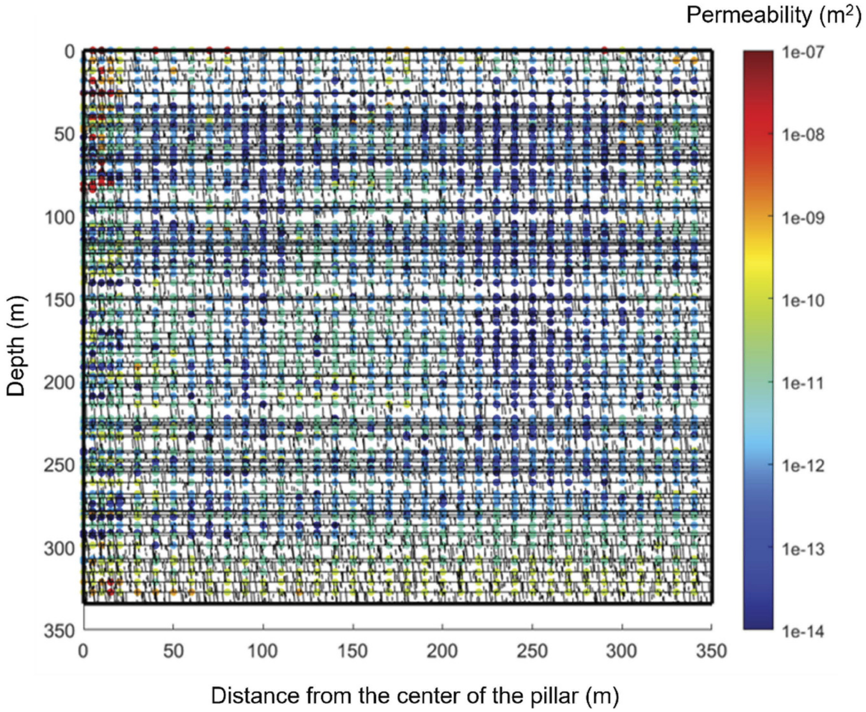

Figure 5. Permeability distribution for deep cover.

The highest permeability under the deep cover is near the edge of panel towards the surface and could be due to the impact of subsidence. Like the shallow-cover site, the strata within 30–40 m from the mine roof have higher permeability compared with the strata above. Apart from these locations, there are multiple extremely low permeability regions/zones in the overburden close to the range of in-situ or undisturbed rock mass. This is a clear distinction between the mining-induced permeability for deep and shallow cover. Based on the difference in induced permeability, it is predicted that the impact of a shale gas casing breach under shallow cover could create more concerns for the mine compared to deep cover. For the shallow and deep cover, Figure 6 shows the exact plot of the permeabilities at about 100 m from the center of the pillar for the stratum directly at the mine roof. The results show the permeability at the edge of the panel (between 15–20 m) is about one to two orders of magnitude greater than the permeability over the abutment pillar (0–15 m). The underlying reasons for permeability differences are the abutment loading and caving process. At the center of the pillar, the loads from retreated panels compact the fractures and reduce their aperture. Approaching the panel edge, bedding plane separation and caved blocks significantly increase the fracture apertures and thus their permeability.

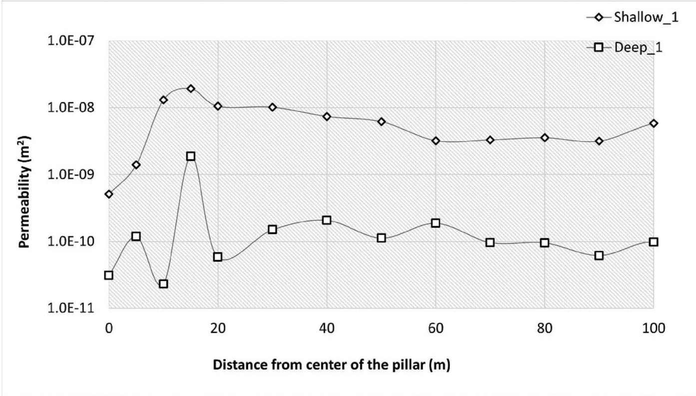

Figure 6. Comparison of permeability for shallow and deep cover.

4 CONCLUSIONS

This study presents the comparison of mining-induced permeability for a deep and shallow site in southwestern Pennsylvania. A discrete fracture network model is developed in FFC with aperture values imported from the geomechanical model in 3DEC. This stochastic DFN model generates 100 realizations to account for potential variation in fracture geometry and the average for each zone is compared. The findings from this study shows that:

i. For both shallow and deep cover, there are notable permeability changes for the strata within 30–40 m of the mine roof, and a shale gas casing breach within this horizon could provide pathways for gas flow toward the mine,
ii. Under shallow cover, the high permeability zone for each stratum at the edge of the panel could extend into the gob to about 100 m and,
iii. Under deep cover, there are multiple locations over the gob with very low permeability values such as in-situ or undisturbed rock mass.

These findings provide insights into the potential impact of a casing breach under different mining depth and could help toward development of best practices for the safe operations of both coal mining and shale gas extraction.

DISCLAIMER

The findings and conclusions in this paper are those of the authors and do not necessarily represent the official position of the National Institute for Occupational Safety and Health, Centers for Disease Control and Prevention. Mention of any company or product does not constitute endorsement by NIOSH.

REFERENCES

Ajayi, K., Khademian, Z., Schatzel, S., Watkins, E. & Gangrade, V. (2021) Numerical modeling of longwall-induced permeability under shallow cover. *Mine Ventilation*. CRC Press.
Ajayi, K., Khademian, Z., Schatzel, S., WATKINS, E. & Gangrade, V. (2022) A Discrete Fracture Network Model for Prediction of Longwall-Induced Permeability. *Mining, Metallurgy & Exploration*, 1–8.
Commonwealth of pennsylvania (1957) Joint Coal and Gas Committee, Gas Well Pillar Study. Harrisburg, Pennsylvania:, Department of Mines and Mineral Industries Oil and Gas Division

Khademian Z., Ajayi, K. M., SU, D. W. H., Schatzel, S. J., Kim, B. H. & Esterhuizen, G. (2022) Rock-mass permeability induced by longwall mining under deep cover: potential gas inflow from a sheared gas well. *SME Annual Conference & Expo*. Utah.

Mine safety and health administration (2018) CFR § 75.323, Title 30, Electronic Code of Federal Regulations. Mineral Resources, Department of Labor.

Pennsylvania department of environmental protection (2022) Longwall Mine Data. https://www.dep.state.pa.us/dep/deputate/minres/LongwallForestlandStudy/Table1.pdf.

Su, D. W., Zhang, P., Van Dyke, M. & Minoski, T. (2018) Effect of Cover Depth on Longwall-Induced Subsurface Deformations and Shale Gas Well Casing Stability. *52nd US Rock Mechanics/Geomechanics Symposium*. American Rock Mechanics Association.

Su, D. W., Zhang, P., Van Dyke, M. & Minoski, T. (2019) Effect of longwall-induced subsurface deformations on shale gas well casing stability under deep covers. *International Journal of Mining Science and Technology*, 29, 3–8.

Watkins E, G. V., Schatzel S, Hollerich C, Addis J (2020) Permeability Determination for Potential Interaction between Shale Gas Wells and the Coal Mine Environment due to Longwall-induced Deformations. *2020 SME Annual Meeting and Exhibit*. Phoenix, AZ.

Watkins, E., Karacan, C. Ö., Gangrade, V. & Schatzel, S. (2021) Assessing Gas Leakage Potential into Coal Mines from Shale Gas Well Failures: Inference from Field Determination of Strata Permeability Responses to Longwall-Induced Deformations. *Natural Resources Research*, 1–14.

Zhang, P., Dougherty, H., su, D. & Trackemas, J. (2019a) Influence of Longwall Mining on the Stability of Gas Wells in Chain Pillars. *Proceedings of the 38th International Conference on Ground Control in Mining*.

Zhang, P., su, D. & Lu, J. (2019b) Influence of Longwall Mining on the Stability of Shale Gas Wells in Barrier Pillars. *American Rock Mechanics Association*. New York.

Zhang, X., Sanderson, D., Harkness, R. & LAST, N. (1996) Evaluation of the 2-D permeability tensor for fractured rock masses. *International journal of rock mechanics and mining sciences & geomechanics abstracts*. Elsevier.